Influence of reactor wall conditions on etch processes in inductively coupled fluorocarbon plasmas

M. Schaepkens, R. C. M. Bosch,[a] T. E. F. M. Standaert, and G. S. Oehrlein[b]
Department of Physics, University at Albany, State University of New York, Albany, New York 12222

J. M. Cook
Lam Research Corporation, Fremont, California 94538-6470

(Received 25 June 1997; accepted 30 January 1998)

The influence of reactor wall conditions on the characteristics of high density fluorocarbon plasma etch processes has been studied. Results obtained during the etching of oxide, nitride, and silicon in an inductively coupled plasma source fed with various feedgases, such as CHF_3, C_3F_6, and C_3F_6/H_2, indicate that the reactor wall temperature is an important parameter in the etch process. Adequate temperature control can increase oxide etch selectivity over nitride and silicon. The loss of fluorocarbon species from the plasma to the walls is reduced as the wall temperature increased. The fluorocarbon deposition on a cooled substrate surface increases concomitantly, resulting in a more efficient suppression of silicon and nitride etch rates, whereas oxide etch rates remain nearly constant. © *1998 American Vacuum Society.* [S0734-2101(98)03504-0]

I. INTRODUCTION

Etching of trenches or contact holes into silicon dioxide is an indispensable process in modern integrated circuit fabrication technology. A high oxide etch rate and etch selectivity of oxide to silicon and nitride are important requirements that need to be met in order for etch processes to be applicable in industrial manufacturing. Etch processes employing low pressure high density fluorocarbon discharges are expected to meet these demands, and have been studied extensively.[1–6]

Low pressure high density fluorocarbon plasma processes, however, have been found to suffer from process drifts.[7] At low pressure, plasma-wall interactions are of significant importance in determining the discharge chemistry. Process drifts have been attributed to changes in reactor wall conditions.[8,9] In order to limit changes in reactor wall conditions and to create a stable and reproducible process environment, it is common in semiconductor processing to ''season'' a reactor. A fundamental understanding of the important mechanisms operating in the conditioning procedure is lacking, however.

This article presents results of a study of the influence of reactor wall conditions on the stability of etch processes. Results obtained during the etching of oxide, nitride, and silicon in an inductively coupled plasma source fed with various feedgases, such as CHF_3, C_3F_6, and C_3F_6/H_2, will be reported. Explanations of the observed effects will be presented.

II. EXPERIMENTAL SETUP

The high-density plasma source used in this work is a radio frequency inductively coupled plasma (ICP) source of planar coil design. This plasma source has also been referred to in literature as transformer coupled plasma (TCP) and radio frequency induction (RFI) source. A schematic outline of the ICP reactor used is shown in Fig. 1. It is similar to the one described by Keller *et al.*[10]

The apparatus consists of an ultrahigh vacuum (UHV) compatible processing chamber in which the plasma source and a wafer holding electrostatic chuck are located. The center part of the ICP source is a planar, 160 mm diameter induction coil that is separated from the process chamber by a 19.6 mm thick, 230 mm diameter quartz window. The coil is powered through a matching network by a 13.56 MHz, 0–2000 W power supply. The results presented here were all obtained at an inductive power level of 1400 W.

A plasma confinement ring that can hold multipole magnets is located below the quartz window. For this work, no magnets were placed into the confinement ring, but the ring itself confines the plasma. The confinement ring has poor thermal contact with other parts of the reactor and its temperature cannot be controlled independently. In the rest of this article, the confinement ring will be referred to as the reactor wall (since this is the surface that the plasma is in contact with). The inner diameter of the confinement ring is 20 cm.

Wafers with diameters of 125 mm are placed on a bipolar electrostatic chuck during processing. The chuck is located 7 cm downstream from the ICP source and allows the wafer to be RF biased and cooled during processing. A helium pressure of 5 Torr is applied to the backside of the wafer during the experiment to achieve a good thermal conduction between the wafer and the chuck.[11] The electrostatic chuck is cooled by a refrigerator. A variable frequency RF power supply (500 kHz–40 MHz, 0–300 W) is used to bias the wafer for etching experiments. The experiments reported in this work were all performed at 3.4 MHz.

Substrates placed at the center of a wafer can be monitored by *in situ* ellipsometry. Plasma diagnostics like a retractable Langmuir probe and optical emission spectroscopy

[a]Permanent address: Eindhoven University of Technology, P.O. Box 513, 5600 MB Eindhoven, The Netherlands.
[b]Electronic mail: oehrlein@cnsibm.albany.edu

IP Bridge Exhibit 2014

DOCKET ALARM Find authenticated court documents without watermarks at docketalarm.com.

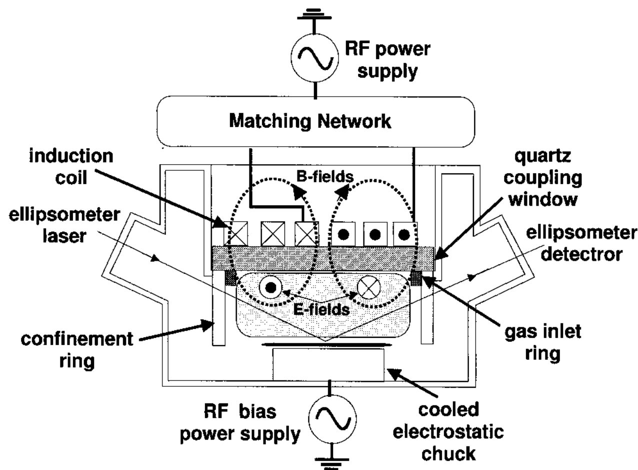

FIG. 1. Schematic of ICP source setup.

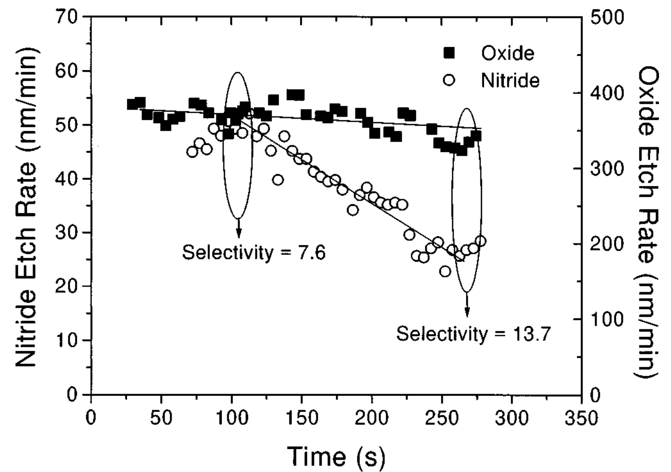

FIG. 2. Nitride etch rate and oxide etch rate as a function of the time that the plasma was switched on (1400 W inductive power, 6 mTorr operating pressure, −100 V self-bias).

(OES) can be used for gas-phase characterization. With the retractable Langmuir probe it is possible to make a scan of the ion current density over 70% of the wafer. The values reported here were measured in the center of the reactor, 2 cm above the wafer surface.

The process chamber is pumped using a 450 ℓ/s turbomolecular pump backed by a Roots blower and a mechanical pump. The process gases are admitted into the reactor through a gas inlet ring located just under the quartz window. The pressure is measured with a capacitance manometer. Pressure control is achieved by an automatic throttle valve in the pump line.

The ICP chamber is connected to a wafer handling cluster system that allows all sample transport to occur under ultrahigh vacuum conditions. Processed samples can be transported from the ICP reactor to a surface analysis chamber for X-ray photoelectron spectroscopy (XPS) without exposure to air.

III. RESULTS AND DISCUSSION

A. Investigation of process drift

It was found in an earlier study by this group that oxide could be etched at a high rate and at the same time selectively to nitride in a C_3F_6/H_2 (40 sccm/15 sccm) discharge at high inductive power (1400 W) and low operating pressure (6 mTorr) when a sufficiently high RF bias power (200 W corresponding to −100 V self-bias) is applied to the wafer.[12] In that study, however, the samples were etched for only a relatively small time period. When etching for longer times, it was observed that etch rates of both oxide and nitride were dependent on the time that the plasma was switched on; see Fig. 2. The nitride etch rate decreases significantly as a function of processing time, whereas the oxide etch rate remains at a near constant value. This results in an increase of oxide-to-nitride selectivity with etching time.

Two time-dependent processes were initially suggested to be responsible for the changes in etch characteristics as a function of time, namely (1) fluorocarbon contamination of the reactor walls during processing and (2) increasing temperature of the reactor. In order to distinguish between these processes, the following experiment was performed; see Fig. 3.

Blanket nitride samples were etched at the same conditions and the rates are plotted versus processing time. Results for three consecutive etch experiments are shown. The first experiment was performed starting with a reactor that has been cleaned with an oxygen plasma prior to the experiment. The reactor is initially at room temperature. In between experiments the reactor was allowed to cool down, but no oxygen plasma cleaning was performed.

It can be seen that during each run there is a significant decrease of the nitride etch rate. The initial value of the etch rate in each run stays at a constant level. This experiment

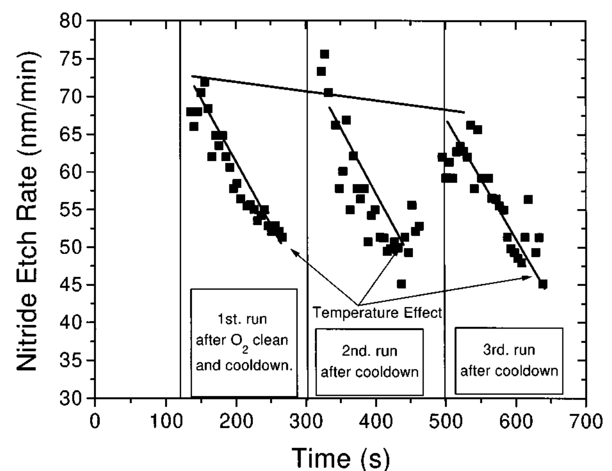

FIG. 3. Nitride etch rate as a function of processing time for three consecutive etch experiments. The first experiment was performed starting with a reactor that has no fluorocarbon material deposited at the walls (reactor was cleaned with an oxygen plasma). Between the etch experiments the reactor was allowed to cool to room temperature, but no oxygen plasma cleaning was performed (1400 W inductive power, 6 mTorr operating pressure, −100 V self-bias).

DOCKET ALARM
Find authenticated court documents without watermarks at docketalarm.com.

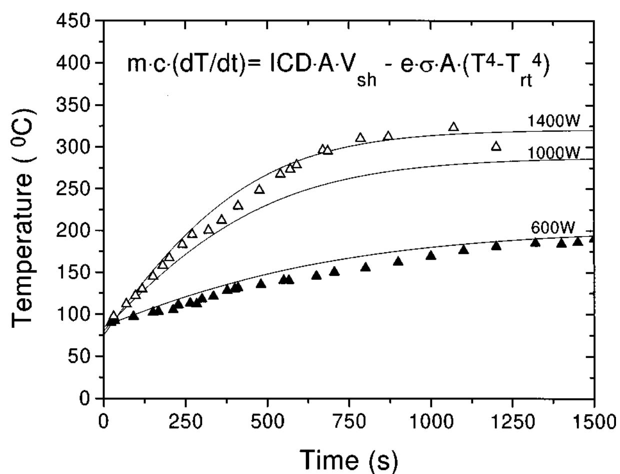

FIG. 4. Wall temperature as a function of processing time. The triangles are experimental data; the curves show the model.

shows that the heating of the reactor is the process that is dominant in producing the observed effect.

B. Time dependence of the reactor wall temperature

The time dependence of the wall temperature has been measured by attaching a thermocouple to the confinement ring. The resulting data for both a 600 and 1400 W C_3F_6/H_2 (40 sccm/15 sccm) plasma at 6 mTorr operating pressure is plotted in Fig. 4. Similar experiments were obtained using different fluorocarbon gases, such as CHF_3 and C_3F_6. The time dependence of the reactor wall temperature changed little with feedgas chemistry.

A simple model that describes the time dependence of the wall temperature T has been developed. In the model it is assumed that the power dissipated in the wall results from collisions of ions with the wall. The ions have an energy equal to the sheath voltage between the floating wall and the plasma. The energy loss factor for the wall is assumed to be Stefan-Boltzmann radiation. The resulting differential equation is

$$m\cdot c\cdot dT/dt=\mathrm{ICD}\cdot A\cdot V_{\mathrm{sh}}-e\cdot\sigma\cdot A\cdot(T^4-T_{\mathrm{RT}}^4), \quad (1)$$

where m is the mass of the confinement ring, c is the heat capacitance of the anodized aluminum confinement ring, ICD is the ion current density, A is the area of reactor wall, V_{sh} is the sheath voltage between the floating wall and the plasma, e is the emissivity of the anodized aluminum confinement ring, σ is the Stefan-Boltzmann constant, and T_{RT} is the room temperature.

The ion current density was measured by Langmuir probe measurement. The sheath voltage was calculated to be 15 V by using an estimated value of 3 eV for the electron temperature. Values between 0.4 and 0.5 for the emissivity were determined from the cooling rate of the wall after the plasma was shut off. The differential equation was solved numerically, resulting in the curves plotted in Fig. 4. The agreement between the model and the experimental data is satisfactory

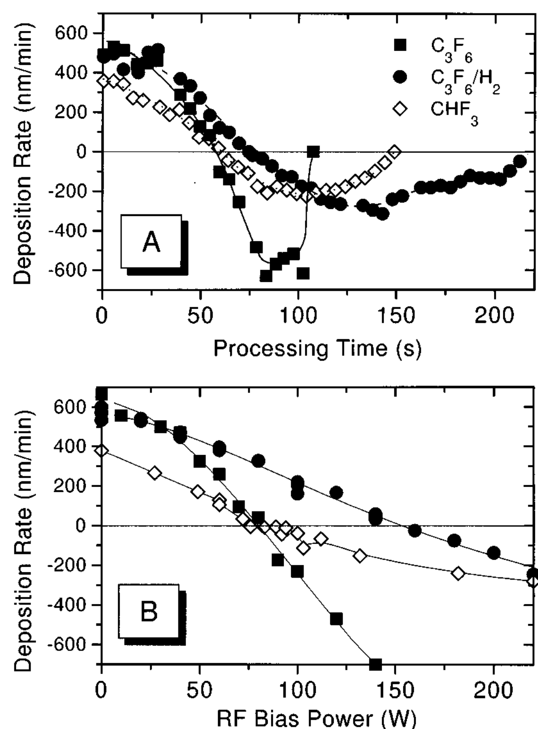

FIG. 5. (A) Passive deposition rates are measured as a function of time on a non-cooled wafer. Three fluorocarbon feedgas chemistries are compared, i.e., CHF_3 (40 sccm), C_3F_6 (40 sccm), and C_3F_6/H_2 (40 sccm/15 sccm) at 1400 W inductive power and 6 mTorr operating pressure. The processing time is proportional to the wafer temperature. For C_3F_6 the 600 W data are also included. The temperature/time correspondence is different in this case. (B) The etch rates of fluorocarbon films deposited at the same conditions at which they are etched are measured as a function of RF bias power at 1400 W inductive power, 6 mTorr operating pressure plasmas fed with various fluorocarbon gases, i.e., CHF_3 (40 sccm), C_3F_6 (40 sccm), and C_3F_6 H_2 (40 sccm/15 sccm).

C. Temperature dependence of plasma–wall interactions

In order to study the temperature dependence of the processes occurring at a non-biased wall that has poor thermal contact, an experiment was performed on a non-biased wafer that is lifted above the chuck by three small Teflon studs. The thermal conductivity between the cooled electrostatic chuck and the wafer is poor in this case. The only energy loss factor is the Stefan-Boltzmann radiation from the wafer to the chuck. Apart from a dissimilarity due to differences in heat capacitance of the wafer and the confinement ring, the behavior of wafer and wall will be similar. The temperature of the wafer will increase with time until it reaches a maximum after which it will no longer change.

Figure 5(A) shows the results of this experiment performed in discharges fed with CHF_3 (40 sccm), C_3F_6 (40 sccm), and C_3F_6/H_2 (40 sccm/15 sccm) using 1400 W inductive power and 6 mTorr operating pressure. The fluorocarbon passive deposition rates are plotted as a function of processing time (i.e., increasing substrate temperature). The initial deposition rates are similar to the deposition rates obtained with a clamped wafer when a helium backside pressure is applied; see Fig. 5(B). As the processing continues, and thus

DOCKET ALARM Find authenticated court documents without watermarks at docketalarm.com.

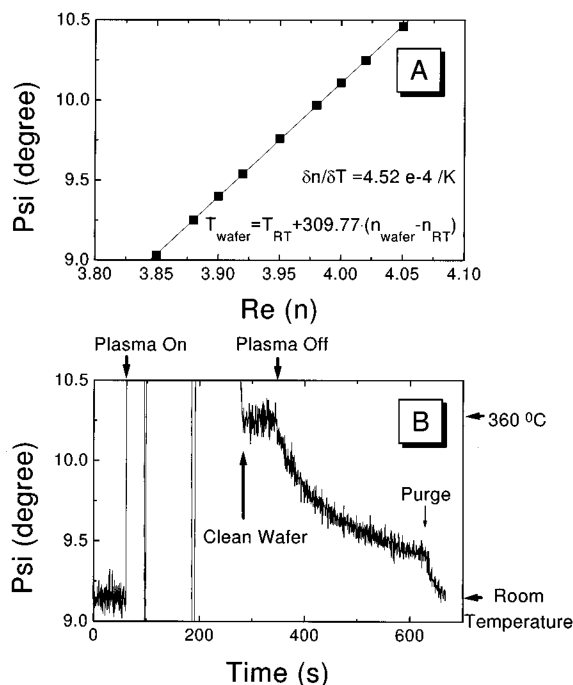

FIG. 6. (A) Simulated correlation between the ellipsometric angle Ψ measured on a crystalline silicon wafer and the real part of the refractive index of the silicon. (B) Ellipsometric angle Ψ measured as a function of time on a non-cooled crystalline silicon wafer in a C_3F_6 plasma at 1400 W inductive power and 6 mTorr operating pressure.

the temperature of the substrate increases, the deposition rate decreases until a point in time where no net deposition takes place. Beyond this point the deposited fluorocarbon material will be removed until no fluorocarbon is left on the *c*-Si wafer. It thus shows that on a surface with a temperature above a certain value no net deposition will take place.

The temperature rise of the non-cooled wafer is quantified by measuring the ellipsometric angle Ψ on the hot, clean *c*-Si wafer after the C_3F_6 experiment from Fig. 5. The Ψ angle is strongly related to the real part of the refractive index, Re(n), of the silicon.[13] The correlation between Ψ and Re(n) is calculated using an ellipsometry simulation routine, and is plotted in Fig. 6(A). Using the temperature coefficient of Re(n) of silicon at 632.8 nm, $\delta n/\delta T = 4.52\times 10^{-4}\ \mathrm{K}^{-1}$, it can be calculated from the data in Fig. 6(B) that the temperature of the wafer, after all fluorocarbon material has been removed, is at a value around 360 °C. This temperature corresponds well with the stable wall temperature in a 1400 W, 6 mTorr plasma; see Fig. 4.

In Fig. 5 it is shown that the point where the net deposition rate is zero occurs earlier in time (i.e., at a lower temperature) for C_3F_6 (40 sccm) than for either CHF_3 (40 sccm), which has a much lower initial deposition rate, or C_3F_6 (40 sccm) with 15 sccm H_2 added to it, which has a similar initial deposition rate.

The results from this experiment allow an interesting analogy to be made between substrate temperature and RF bias power when etching fluorocarbon material deposited on a cooled wafer. The etch rate of fluorocarbon material (deposited at the same condition as etching is performed) as a function of RF bias power is plotted in Fig. 5(B). It shows that C_3F_6 has a lower threshold RF bias power for etching than C_3F_6/H_2 even though the passive deposition rates (i.e., 0 W RF bias power) are similar. It also shows that CHF_3 has a higher threshold RF bias power than C_3F_6, even though the passive deposition rate is significantly lower. From this comparison it can be suggested that, in fluorocarbon etching, the RF bias power and the substrate temperature play a similar role, i.e., an energy source for enabling chemical reactions. It further shows that the transition from deposition to etching is strongly dependent on the feedgas chemistry. The reason why CHF_3 and C_3F_6/H_2 deposited fluorocarbon films require a higher threshold RF bias power or a higher substrate temperature is due to differences in chemical composition. The F/C ratios of the CHF_3 and C_3F_6/H_2 fluorocarbon films are lower than the F/C ratio of C_3F_6 fluorocarbon material due to the fluorine scavenging effect of hydrogen.[12,14]

D. Temperature dependence of the gas phase chemistry

The results from Sec. III C indicate that fluorocarbon species that are precursors for deposition on low temperature surfaces do not deposit on hot surfaces and remain in the plasma. The (low temperature surface) deposition precursor density thus increases. This is consistent with results from Chinzei *et al.*,[15] who reported that in a C_4F_8 ICP no polymer deposition occurs on surfaces at temperatures higher than 200 °C. The density of CF and CF_2 radicals, as measured by mass spectrometry, is one order of magnitude higher in a 200 °C heated reactor in comparison to a reactor at 30 °C. Hikosaka *et al.*[16] also reported mass spectrometric results showing that, as the temperature of their quartz wall increased, the CF_3 radical density increased due to a reduced surface loss of these species. They additionally found an increased CO density due to enhanced etching of the quartz wall at higher temperatures and a decrease in *F* density which they ascribed to the enhanced F absorption on the quartz wall. Fluorine absorption by an aluminum wall has also been reported by Chinzei *et al.* In mass spectrometry measurements Maruyama *et al.*[17] observed that for CF_4 plasmas an increase in the CF_x radical density occurs as the wall temperature goes up. O'Neill and Singh[9] who performed ultraviolet (UV)-absorption spectroscopy in order to examine the CF_2 radical density in a C_2F_6/CF_4 plasma also reported a steady increase of this density as processing proceeds. They ascribed this effect to increasing polymer deposition on the wall, but also mentioned that the reactor wall temperature may play a significant role.

Figure 7 shows optical emission spectra taken on a 1400 W, 6 mTorr, 40 sccm C_3F_6 discharge in both a relatively cold (60 °C) and a hot (300 °C) reactor. Significant intensity differences can be observed in the emission from various carbon containing species. In Fig. 8 the peak intensities of CF_2, C_2, CO and also those of atomic fluorine and oxygen are plotted as a function of reactor wall temperature. The intensities are normalized to their value in a hot reactor.

It shows that the initial value, i.e., in a cold reactor, of the

DOCKET ALARM Find authenticated court documents without watermarks at docketalarm.com.

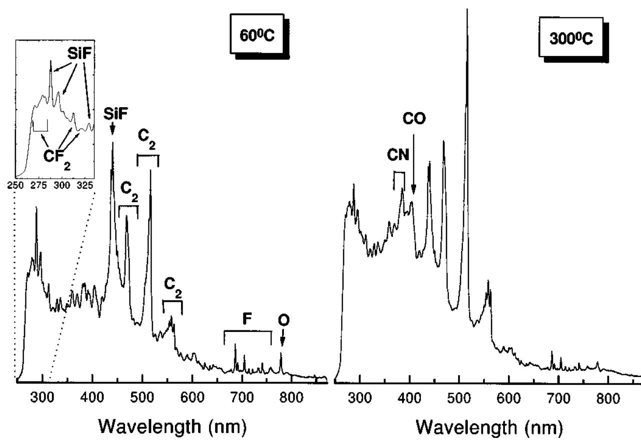

FIG. 7. Comparison of optical emission spectra measured on a C_3F_6 plasma at 1400 W inductive power and 6 mTorr operating pressure. The left panel shows the spectrum measured in a cold (60 °C) reactor and the right panel shows the spectrum measured in a hot (300 °C) reactor.

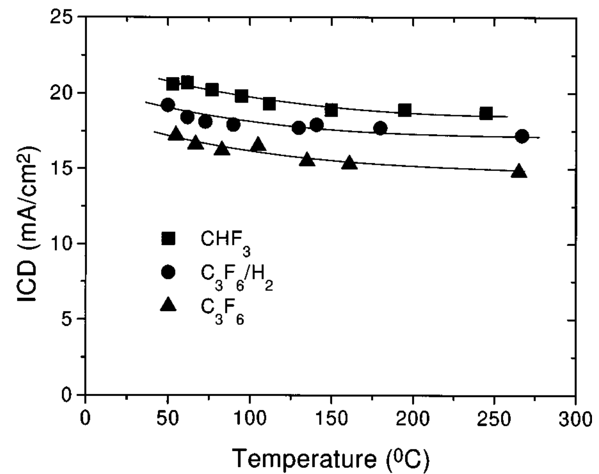

FIG. 9. Ion current density as a function of reactor wall temperature (1400 W inductive power, 6 mTorr operating pressure).

intensity of carbon containing species is around 50%–60% of the final, hot reactor value. The fluorine intensity is initially 10% higher than its final intensity. This indicates that the concentration ratio of carbon containing species, i.e., deposition precursors, over atomic fluorine, i.e., etch precursor, increases as the reactor temperature increases.

The increase in the CO intensity coincides with a decrease of the atomic oxygen signal. The CO formation can therefore be explained by an increased carbon density in the plasma reacting with atomic oxygen.

At a constant pressure, the particle density decreases as the reactor temperature increases. Therefore, the electron mean free path and thus the electron temperature will increase. The constant emission intensity at temperatures higher than 200 °C may therefore correspond to a decreasing radical density. A change in the electron temperature, however, should not influence the relative intensity of F emission to CF_2 and C_2, i.e., the gas phase F/C ratio, assuming approximately similar excitation cross sections for these species.

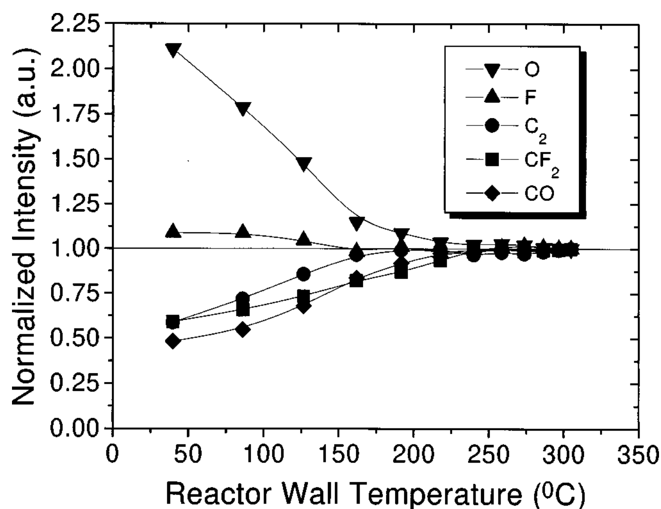

FIG. 8. Emission intensities measured in a C_3F_6 plasma at 1400 W inductive power and 6 mTorr operating pressure. The intensities of the various species are normalized to their value in a hot reactor.

E. Temperature dependence of the ion current density

The ion current density has been measured as a function of reactor wall temperature in CHF_3, C_3F_6, and C_3F_6/H_2 discharges; see Fig. 9. The ion current density decreases as the wall temperature increases. The ion density may decrease more significantly as a function of reactor wall temperature than the ion current density does, assuming that the electron temperature increases. A higher electron temperature leads to an increase in the ion acoustic velocity, which results in a higher ion current density for a given ion density.

The decrease in the ion density can partially be explained by the fact that the overall particle density goes down as the temperature of the reactor walls increases.

F. Temperature dependence of plasma-surface interactions

1. Fluorocarbon deposition

The results previously presented suggest a time dependence of the fluorocarbon deposition on cold surfaces, such as cooled substrates. Figure 10 shows the passive fluorocarbon deposition measured as a function of reactor wall temperature in a C_3F_6 (40 sccm) and C_3F_6/H_2 (40 sccm/12 sccm) plasma at 1400 W inductive power and 6 mTorr operating pressure. The deposition rate shows a maximum as a function of wall temperature. This can be explained as follows.

Initially passive deposition will take place on the walls at the same rate as on the wafer. As the walls heat up, the passive deposition rate on the walls will decrease and ultimately fluorocarbon removal will occur. The deposition precursor density in the gas phase increases at the same time, raising the passive deposition on the cooled wafer. After all the fluorocarbon material has been removed from the walls, the deposition precursor density in the gas phase and thus the

DOCKET ALARM Find authenticated court documents without watermarks at docketalarm.com.

DOCKET ALARM

Explore Litigation Insights

Docket Alarm provides insights to develop a more informed litigation strategy and the peace of mind of knowing you're on top of things.

Real-Time Litigation Alerts

Keep your litigation team up-to-date with **real-time alerts** and advanced team management tools built for the enterprise, all while greatly reducing PACER spend.

Our comprehensive service means we can handle Federal, State, and Administrative courts across the country.

Advanced Docket Research

With over 230 million records, Docket Alarm's cloud-native docket research platform finds what other services can't. Coverage includes Federal, State, plus PTAB, TTAB, ITC and NLRB decisions, all in one place.

Identify arguments that have been successful in the past with full text, pinpoint searching. Link to case law cited within any court document via Fastcase.

Analytics At Your Fingertips

Learn what happened the last time a particular judge, opposing counsel or company faced cases similar to yours.

Advanced out-of-the-box PTAB and TTAB analytics are always at your fingertips.

API

Docket Alarm offers a powerful API (application programming interface) to developers that want to integrate case filings into their apps.

LAW FIRMS

Build custom dashboards for your attorneys and clients with live data direct from the court.

Automate many repetitive legal tasks like conflict checks, document management, and marketing.

FINANCIAL INSTITUTIONS

Litigation and bankruptcy checks for companies and debtors.

E-DISCOVERY AND LEGAL VENDORS

Sync your system to PACER to automate legal marketing.

WHAT WILL YOU BUILD? | sales@docketalarm.com | 1-866-77-FASTCASE

fastcase®
Smarter legal research.